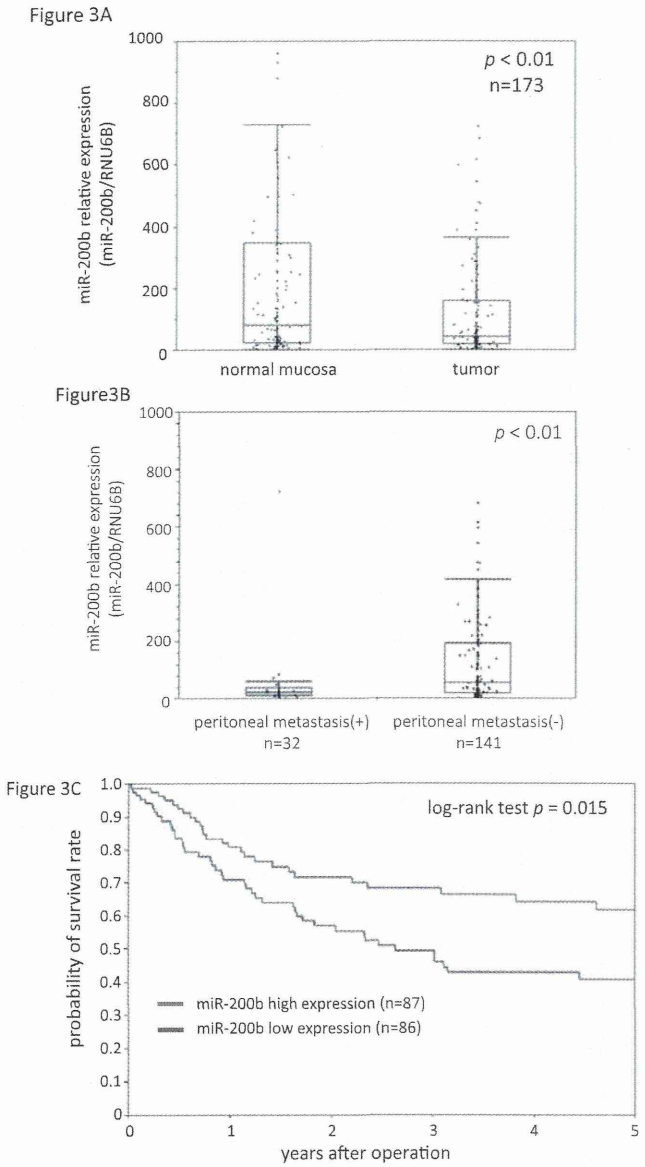

Fig. 3. Expression status of miR-200b and Kaplan–Meier survival curves in gastric cancer patients. (**A**) The mean expression levels of miR-200b in cancerous tissue specimens were significantly lower than those in non-cancerous tissues ($P < 0.01$). (**B**) The mean expression levels of miR-200b in the cancerous tissue specimens of patients with peritoneal metastasis ($n = 32$) were significantly lower than those without peritoneal metastasis ($n = 141$) ($P < 0.01$). (**C**) The overall survival curves are presented according to the expression level of miR-200b in gastric cancer patients. Patients with low miR-200b expression ($n = 86$) had a poorer prognosis than those with high expression ($n = 87$) (log-rank test; $P = 0.015$).

expression in the stroma of gastric cancer, and the patients with high α-SMA expression showed methylation of the miR-200b promoter. These findings suggest that CAFs stimulate cancer invasion and migration via epigenetic changes of miR-200b in gastric cancer. Moreover, model mice with peritoneal dissemination showed methylated miR-200b and low miR-200b expression. Similarly, we found that patients with low miR-200b expression had a significantly poorer prognosis than those with high miR-200b expression, and low miR-200b expression was associated with peritoneal dissemination.

This is the first study to directly analyze the role of CAFs to regulate the expression of miRNA via epigenetic changes to the best of our knowledge. The CAFs populations in tumor-associated stroma are known to include both fibroblasts and myofibroblasts. Myofibroblasts are endowed with the ability to promote tumor growth and are associated with higher grade malignancy and poorer prognosis in patients with several cancers (26,33,34). Indeed, the CAFs prepared and examined in our study contained a subpopulation of α-SMA-expressing fibroblasts, as indicated by immunohistochemistry (Figure 4 and Supplementary Figure 2, available at *Carcinogenesis* Online). CAFs can promote cancer progression, invasion and metastasis by modulating multiple components in the cancer niche to build a permissive and supportive microenvironment for tumor growth and invasion through the secretion of growth factors including hepatocyte growth factor, stromal cell-derived factor-1, several chemokine factors, platelet-derived growth factor, fibroblast growth factor and transforming growth factor (TGF)-β (35–38). In particular, TGF-β from tumor-associated stroma is an important factor for the induction and functional activation of EMT-related pathways (39–41). Interestingly, TGF-β was shown to induce the expression of DNA methyltransferases, which function in DNA methylation, in several cancers (42–44). Moreover, TGF-β also mediates these effects through the action of epigenetic switches such as CD133 and tristetrapolin, as well as miR-200 CpG island methylation events (18,42,45). Thus, in this study, some signals from CAFs, such as TGF-β, might be related to the corresponding methylation changes observed in miR-200b. This aspect remains to be investigated in future research.

Members of the miR-200 family are being increasingly recognized as important players for regulating epithelial characteristics of cells through direct targeting of *ZEB1* and *ZEB2*, which are EMT-inducing transcription factors, via transcriptional repression of E-cadherin expression (13,46); our present results in gastric cancer cell lines confirm this role of miR-200 (Supplementary Figure 2A–E, available at *Carcinogenesis* Online). Based on the EMT hypothesis of cancer metastasis, low expression of the miR-200 family would lead to increased metastasis through the targeted induction of *ZEB1* and *ZEB2* expression, resulting in repressed E-cadherin expression and the adoption of mesenchymal characteristics. This EMT process has been shown to occur in several types of cancer cells, whereby lower levels of the miR-200 family have been associated with a higher frequency of invasive and metastatic tumors and a poorer prognosis (16,46–48). However, several studies have also shown the opposite effect of high expression of miR-200 family members enhancing distant metastases through promoting secondary cancer colonization (30,49,50) in the mesenchymal–epithelial transition process. This has been interpreted as a potential requirement for EMT to accomplish the first steps of metastasis, and a reversion (mesenchymal–epithelial transition) to accomplish the final step of colonization. EMT is first acquired in the onset of transmigration and then reversed mesenchymal–epithelial transition occurs in the new colony; this process is described as epithelial–mesenchymal plasticity. However, because peritoneal dissemination is the most common cause of death in gastric cancer, a better understanding of the EMT mechanism is critical for developing new treatments that can improve the survival of gastric cancer patients with peritoneal dissemination. During EMT, methylation-induced downregulation of miR-200b allows upregulation of several of its direct target genes, including *ZEB1* and *ZEB2*, as they increase invasive and metastatic potential, involving the simultaneous loss of E-cadherin and enhancement of Vimentin expression at peritoneal dissemination sites. Our results demonstrated that restoration of miR-200b expression is a potential candidate approach for miRNA-based therapy against peritoneal dissemination of gastric cancer.

In conclusion, this study provides important insight supporting the roles of miR-200b during peritoneal dissemination in gastric cancer. Our discovery of the pivotal role that miR-200b plays in the metastatic behavior of gastric cancer indicates that this miRNA has potential value as a diagnostic and prognostic biomarker. These results may also have implications for the clinical management of patients with peritoneal dissemination.

Table II. miR-200b expression and clincopathological features

Features	Total (n = 173)	miR-200b				P-value
		High expression, n = 87 (%)		Low expression, n = 86 (%)		
Age (years)						0.764
Mean ± SD	65.9±11.2	67.0±11.8		65.5±11.1		
Gender						0.955
Male	111	56	64.4	55	63.9	
Female	62	31	35.6	31	36.1	
Differentiation						0.002*
Well/moderate	79	50	57.5	29	33.7	
Poor/other	94	37	42.5	57	66.3	
Depth of tumor invasion						0.010*
T1–2	54	35	40.3	19	22.1	
T3–4	119	52	59.7	67	77.9	
Lymph node metastasis						0.119
Absent	58	34	39.1	24	27.9	
Present	115	53	60.9	62	72.1	
Lymphatic invasion						0.670
Absent	59	31	35.6	28	32.6	
Present	114	56	64.4	58	67.4	
Venous invasion						0.017*
Absent	121	68	78.2	53	61.6	
Present	52	19	21.8	33	38.4	
Peritoneal metastasis						<0.001*
Absent	141	80	92.0	61	70.9	
Present	32	7	8.0	25	29.1	
Distant metastasis						0.002*
Absent	127	73	83.9	54	62.8	
Present	46	14	16.1	32	37.2	
Stage						0.005*
I–II	91	55	63.2	36	41.9	
III–IV	82	32	36.8	50	58.1	

Staging was classified by Union for International Cancer Control, seventh edition.
*P-value < 0.05.

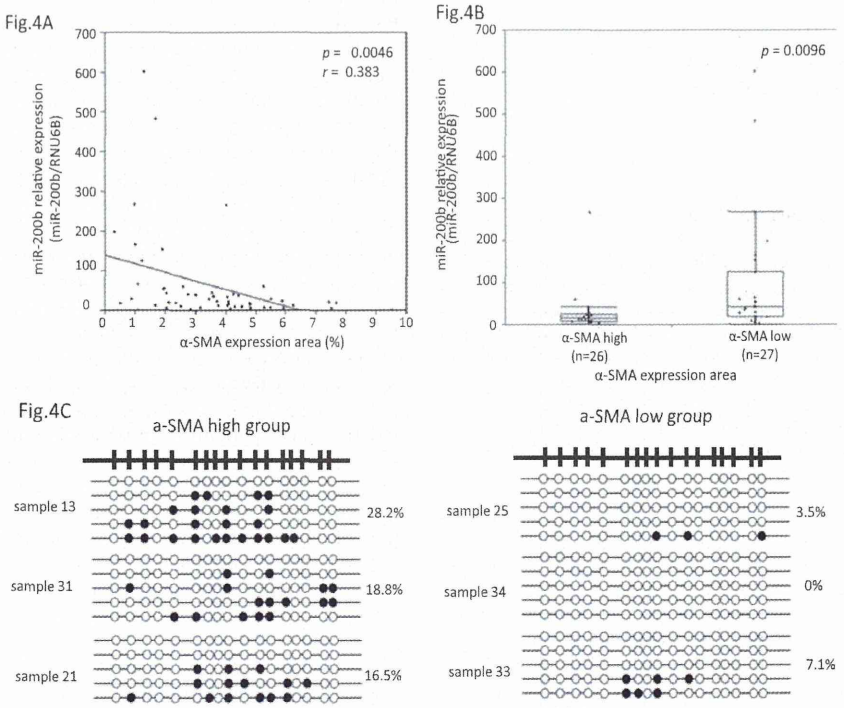

Fig. 4. Relationship of methylation status of miR-200b and CAFs expression in gastric cancer specimens. (**A**) There was a significant inverse correlation between miR-200b expression and the α-SMA score. (**B**) Patients with high α-SMA expression had significantly lower miR-200b expression than low α-SMA patients. (**C**) We chose three low miR-200b/high α-SMA score patients and three high miR-200b/low α-SMA score patients for methylation analysis. The CpG islands were more significantly methylated in the low miR-200b/high α-SMA group than the high miR-200b/low α-SMA group.

Supplementary material

Supplementary Tables 1–3 and Figures 1–4 can be found at http://carcin.oxfordjournals.org/

Funding

Grants-in-Aid for Scientific Research of MEXT (24008081, 25430111, 25461953, 25861199, 25861200, 24592005 and 21229015); Funding Program for Next Generation World Leading Researchers (LS094); Grants-in-Aid for Scientific Research on Innovative Areas of MEXT 'Systems Cancer Research' (4201); The MEXT Strategic Programs on Innovative Research 'Supercomputational Life Science'. This research used computational resources of the K computer provided by the RIKEN Advanced Institute for Computational Science through the HPCI System Research project (Project ID: hp140230). Computation time was also provided by the Supercomputer System, Human Genome Center, Institute of Medical Science, University of Tokyo and The OITA Cancer Research Foundation 2014. Grant-in-Aid for Scientific Research of Ministry of Health, Labour and Welfare (14524362 and 14525288).

Acknowledgements

We thank Ms M.Kasagi, Ms T.Kawano and Ms K.Oda for their excellent technical assistance.

Conflict of Interest Statement: None declared.

References

1. Ikeguchi,M. *et al.* (2009) Recent results of therapy for scirrhous gastric cancer. *Surg. Today*, **39**, 290–294.
2. Takahashi,I. *et al.* (2000) Clinicopathological features of long-term survivors of scirrhous gastric cancer. *Hepatogastroenterology*, **47**, 1485–1488.
3. Joyce,J.A. *et al.* (2009) Microenvironmental regulation of metastasis. *Nat. Rev. Cancer*, **9**, 239–252.
4. De Wever,O. *et al.* (2008) Stromal myofibroblasts are drivers of invasive cancer growth. *Int. J. Cancer*, **123**, 2229–2238.
5. Bhowmick,N.A. *et al.* (2004) Stromal fibroblasts in cancer initiation and progression. *Nature*, **432**, 332–337.
6. Hwang,R.F. *et al.* (2008) Cancer-associated stromal fibroblasts promote pancreatic tumor progression. *Cancer Res.*, **68**, 918–926.
7. Grugan,K.D. *et al.* (2010) Fibroblast-secreted hepatocyte growth factor plays a functional role in esophageal squamous cell carcinoma invasion. *Proc. Natl Acad. Sci. USA*, **107**, 11026–11031.
8. Yashiro,M. *et al.* (2010) Cancer-stromal interactions in scirrhous gastric carcinoma. *Cancer Microenviron.*, **3**, 127–135.
9. Fuyuhiro,Y. *et al.* (2012) Cancer-associated orthotopic myofibroblasts stimulates the motility of gastric carcinoma cells. *Cancer Sci.*, **103**, 797–805.
10. De Craene,B. *et al.* (2013) Regulatory networks defining EMT during cancer initiation and progression. *Nat. Rev. Cancer*, **13**, 97–110.
11. van Kouwenhove,M. *et al.* (2011) MicroRNA regulation by RNA-binding proteins and its implications for cancer. *Nat. Rev. Cancer*, **11**, 644–656.
12. Korpal,M. *et al.* (2008) The miR-200 family inhibits epithelial-mesenchymal transition and cancer cell migration by direct targeting of E-cadherin transcriptional repressors ZEB1 and ZEB2. *J. Biol. Chem.*, **283**, 14910–14914.
13. Gregory,P.A. *et al.* (2008) The miR-200 family and miR-205 regulate epithelial to mesenchymal transition by targeting ZEB1 and SIP1. *Nat. Cell Biol.*, **10**, 593–601.
14. Kurashige,J. *et al.* (2012) MicroRNA-200b regulates cell proliferation, invasion, and migration by directly targeting ZEB2 in gastric carcinoma. *Ann. Surg. Oncol.*, **19** (suppl. 3), S656–S664.
15. Wellner,U. *et al.* (2009) The EMT-activator ZEB1 promotes tumorigenicity by repressing stemness-inhibiting microRNAs. *Nat. Cell Biol.*, **11**, 1487–1495.
16. Yu,J. *et al.* (2010) MicroRNA, hsa-miR-200c, is an independent prognostic factor in pancreatic cancer and its upregulation inhibits pancreatic cancer invasion but increases cell proliferation. *Mol. Cancer*, **9**, 169.
17. Xia,H. *et al.* (2010) miR-200a regulates epithelial-mesenchymal to stem-like transition via ZEB2 and beta-catenin signaling. *J. Biol. Chem.*, **285**, 36995–37004.
18. Davalos,V. *et al.* (2012) Dynamic epigenetic regulation of the microRNA-200 family mediates epithelial and mesenchymal transitions in human tumorigenesis. *Oncogene*, **31**, 2062–2074.
19. Tellez,C.S. *et al.* (2011) EMT and stem cell-like properties associated with miR-205 and miR-200 epigenetic silencing are early manifestations during carcinogen-induced transformation of human lung epithelial cells. *Cancer Res.*, **71**, 3087–3097.
20. Li,A. *et al.* (2010) Pancreatic cancers epigenetically silence SIP1 and hypomethylate and overexpress miR-200a/200b in association with elevated circulating miR-200a and miR-200b levels. *Cancer Res.*, **70**, 5226–5237.
21. Yashiro,M. *et al.* (1995) Establishment of two new scirrhous gastric cancer cell lines: analysis of factors associated with disseminated metastasis. *Br. J. Cancer*, **72**, 1200–1210.
22. Yashiro,M. *et al.* (1996) Peritoneal metastatic model for human scirrhous gastric carcinoma in nude mice. *Clin. Exp. Metastasis*, **14**, 43–54.
23. Yanagihara,K. *et al.* (2005) Development and biological analysis of peritoneal metastasis mouse models for human scirrhous stomach cancer. *Cancer Sci.*, **96**, 323–332.
24. Iwaya,T. *et al.* (2012) Downregulation of miR-144 is associated with colorectal cancer progression via activation of mTOR signaling pathway. *Carcinogenesis*, **33**, 2391–2397.
25. Nishida,N. *et al.* (2012) MicroRNA-10b is a prognostic indicator in colorectal cancer and confers resistance to the chemotherapeutic agent 5-fluorouracil in colorectal cancer cells. *Ann. Surg. Oncol.*, **19**, 3065–3071.
26. Tsujino,T. *et al.* (2007) Stromal myofibroblasts predict disease recurrence for colorectal cancer. *Clin. Cancer Res.*, **13**, 2082–2090.
27. Zhang,Y. *et al.* (2011) Ovarian cancer-associated fibroblasts contribute to epithelial ovarian carcinoma metastasis by promoting angiogenesis, lymphangiogenesis and tumor cell invasion. *Cancer Lett.*, **303**, 47–55.
28. Yanagihara,K. *et al.* (2006) A photon counting technique for quantitatively evaluating progression of peritoneal tumor dissemination. *Cancer Res.*, **66**, 7532–7539.
29. Yanagihara,K. *et al.* (2004) Establishment of two cell lines from human gastric scirrhous carcinoma that possess the potential to metastasize spontaneously in nude mice. *Cancer Sci.*, **95**, 575–582.
30. Hur,K. *et al.* (2013) MicroRNA-200c modulates epithelial-to-mesenchymal transition (EMT) in human colorectal cancer metastasis. *Gut*, **62**, 1315–1326.
31. Bracken,C.P. *et al.* (2008) A double-negative feedback loop between ZEB1-SIP1 and the microRNA-200 family regulates epithelial-mesenchymal transition. *Cancer Res.*, **68**, 7846–7854.
32. Neves,R. *et al.* (2010) Role of DNA methylation in miR-200c/141 cluster silencing in invasive breast cancer cells. *BMC Res. Notes*, **3**, 219.
33. Navab,R. *et al.* (2011) Prognostic gene-expression signature of carcinoma-associated fibroblasts in non-small cell lung cancer. *Proc. Natl Acad. Sci. USA*, **108**, 7160–7165.
34. Finak,G. *et al.* (2008) Stromal gene expression predicts clinical outcome in breast cancer. *Nat. Med.*, **14**, 518–527.
35. Orimo,A. *et al.* (2005) Stromal fibroblasts present in invasive human breast carcinomas promote tumor growth and angiogenesis through elevated SDF-1/CXCL12 secretion. *Cell*, **121**, 335–348.
36. Tsuyada,A. *et al.* (2012) CCL2 mediates cross-talk between cancer cells and stromal fibroblasts that regulates breast cancer stem cells. *Cancer Res.*, **72**, 2768–2779.
37. Okabe,H. *et al.* (2012) Identification of CXCL5/ENA-78 as a factor involved in the interaction between cholangiocarcinoma cells and cancer-associated fibroblasts. *Int. J. Cancer*, **131**, 2234–2241.
38. Bhowmick,N.A. *et al.* (2004) TGF-beta signaling in fibroblasts modulates the oncogenic potential of adjacent epithelia. *Science*, **303**, 848–851.
39. Zavadil,J. *et al.* (2005) TGF-beta and epithelial-to-mesenchymal transitions. *Oncogene*, **24**, 5764–5774.
40. Pardali,K. *et al.* (2007) Actions of TGF-beta as tumor suppressor and pro-metastatic factor in human cancer. *Biochim. Biophys. Acta*, **1775**, 21–62.
41. Xu,J. *et al.* (2009) TGF-beta-induced epithelial to mesenchymal transition. *Cell Res.*, **19**, 156–172.
42. You,H. *et al.* (2010) Epigenetic regulation of cancer stem cell marker CD133 by transforming growth factor-beta. *Hepatology*, **51**, 1635–1644.
43. Zhang,Q. *et al.* (2011) TGF-β regulates DNA methyltransferase expression in prostate cancer, correlates with aggressive capabilities, and predicts disease recurrence. *PLoS One*, **6**, e25168.
44. Matsumura,N. *et al.* (2011) Epigenetic suppression of the TGF-beta pathway revealed by transcriptome profiling in ovarian cancer. *Genome Res.*, **21**, 74–82.
45. Sohn,B.H. *et al.* (2010) Functional switching of TGF-beta1 signaling in liver cancer via epigenetic modulation of a single CpG site in TTP promoter. *Gastroenterology*, **138**, 1898–1908.

46. Park,S.M. *et al.* (2008) The miR-200 family determines the epithelial phenotype of cancer cells by targeting the E-cadherin repressors ZEB1 and ZEB2. *Genes Dev.*, **22**, 894–907.
47. Gibbons,D.L. *et al.* (2009) Contextual extracellular cues promote tumor cell EMT and metastasis by regulating miR-200 family expression. *Genes Dev.*, **23**, 2140–2151.
48. Ceppi,P. *et al.* (2010) Loss of miR-200c expression induces an aggressive, invasive, and chemoresistant phenotype in non-small cell lung cancer. *Mol. Cancer Res.*, **8**, 1207–1216.
49. Korpal,M. *et al.* (2011) Direct targeting of Sec23a by miR-200s influences cancer cell secretome and promotes metastatic colonization. *Nat. Med.*, **17**, 1101–1108.
50. Dykxhoorn,D.M. *et al.* (2009) miR-200 enhances mouse breast cancer cell colonization to form distant metastases. *PLoS One*, **4**, e7181.

Received May 12, 2014; revised September 28, 2014; accepted November 11, 2014

Role of pyruvate kinase M2 in transcriptional regulation leading to epithelial–mesenchymal transition

Atsushi Hamabe[a,b,1], Masamitsu Konno[b,1], Nobuhiro Tanuma[c], Hiroshi Shima[c], Kenta Tsunekuni[a,d,e], Koichi Kawamoto[a,b], Naohiro Nishida[b], Jun Koseki[e], Koshi Mimori[f], Noriko Gotoh[g], Hirofumi Yamamoto[a], Yuichiro Doki[a,b,e], Masaki Mori[a,b,e,2], and Hideshi Ishii[b,e,2]

Departments of [a]Gastrointestinal Surgery and [b]Frontier Science for Cancer and Chemotherapy, Graduate School of Medicine, Osaka University, Osaka 565-0871, Japan; [c]Division of Cancer Chemotherapy, Miyagi Cancer Center Research Institute, Sendai 981-1293, Japan; [d]Taiho Pharmaceutical Co., Ltd., Chiyoda-ku, Tokyo 101-0054, Japan; [e]Department of Cancer Profiling Discovery, Graduate School of Medicine, Osaka University, Osaka 565-0871, Japan; [f]Department of Surgery, Kyushu University Beppu Hospital, Beppu 874-0838, Japan; and [g]Division of Cancer Cell Biology, Cancer Research Institute of Kanazawa University, Kanazawa 920-1192, Japan

Edited by Carlo M. Croce, The Ohio State University, Columbus, OH, and approved September 25, 2014 (received for review May 2, 2014)

Pyruvate kinase M2 (PKM2) is an alternatively spliced variant of the pyruvate kinase gene that is preferentially expressed during embryonic development and in cancer cells. PKM2 alters the final rate-limiting step of glycolysis, resulting in the cancer-specific Warburg effect (also referred to as aerobic glycolysis). Although previous reports suggest that PKM2 functions in nonmetabolic transcriptional regulation, its significance in cancer biology remains elusive. Here we report that stimulation of epithelial–mesenchymal transition (EMT) results in the nuclear translocation of PKM2 in colon cancer cells, which is pivotal in promoting EMT. Immunoprecipitation and LC-electrospray ionized TOF MS analyses revealed that EMT stimulation causes direct interaction of PKM2 in the nucleus with TGF-β–induced factor homeobox 2 (TGIF2), a transcriptional cofactor repressor of TGF-β signaling. The binding of PKM2 with TGIF2 recruits histone deacetylase 3 to the E-cadherin promoter sequence, with subsequent deacetylation of histone H3 and suppression of E-cadherin transcription. This previously unidentified finding of the molecular interaction of PKM2 in the nucleus sheds light on the significance of PKM2 expression in cancer cells.

pyruvate kinase M2 | epithelial–mesenchymal transition | colorectal cancer | invasion | transforming growth factor-β–induced factor homeobox 2

Colorectal cancer (CRC) is the second most common cancer in the world, with more than 1.2 million new cases and about 600,000 deaths annually (1). Cancerous cells exploit a cancer-specific glycolytic system known as the Warburg effect (also referred to as aerobic glycolysis), which involves rapid glucose uptake and preferential conversion to lactate, despite an abundance of oxygen (2, 3). The precise mechanism underpinning aerobic glycolysis was unclear for a long time. However, in 2008, pyruvate kinase M2 (PKM2) gained attention when its expression was shown to be required for the maintenance of aerobic glycolysis (4). PKM2 is an alternatively spliced variant of the PKM gene that regulates the final rate-limiting step of glycolysis. PKM2 is expressed during embryonic development, but it is generally not expressed in most adult tissues. However, its counterpart, PKM1, is exclusively expressed in adult tissues. PKM2 has been shown to be reactivated in tumor development (5, 6). In cancer cells, PKM2 expression allows the diversion of glycolytic flux into the pentose phosphate pathway associated with attenuated pyruvate kinase activity, thereby meeting the biosynthetic demands for rapid proliferation (3).

Investigations about the nuclear function of PKM2 arose after elucidation of the PKM2 metabolic function. It was identified that in cancer cells, PKM2 can translocate into the nucleus and function as a transcriptional cofactor in response to several extracellular signals, including EGF and hypoxia, subsequently activating CYCLIN D1, C-MYC, or hypoxia-inducible factor 1α (HIF-1α) (7, 8). Particularly in the hypoxic condition, PKM2 interacts with HIF-1α and participates in a positive feedback loop, thereby enhancing HIF-1α transactivation and reprogramming glucose metabolism by regulating the expression of glycolysis-associated enzymes (8). This finding suggested that the PKM2 nuclear function may operate upstream of metabolic regulation and that the resultant metabolic reprogramming and oncogene activation by PKM2 work cooperatively to promote cancer cell proliferation and tumor growth.

In addition to proliferation maintenance and growth suppression prevention, invasion and metastasis have also been targeted as hallmarks of cancer (9). In the invasion process, cancer cells acquire the ability to dissociate from the bulk of the tumor and to migrate into the surrounding stroma, which is regulated by epithelial–mesenchymal transition (EMT) (9, 10). During EMT, cancer cells lose their cell-to-cell contacts by

Significance

Our study shows that pyruvate kinase M2 (PKM2), an alternatively spliced variant of the pyruvate kinase gene, mediates epithelial–mesenchymal transition (EMT), which is critical for cancer cells to acquire invasive potential. Our study demonstrates that EMT stimulates nuclear translocation of PKM2 and decreases epithelial cadherin transcription (a requirement for EMT induction). Our results also demonstrate that PKM2 interacts with the transcriptional factor TGF-β–induced factor homeobox 2, which induces the deacetylation of histone H3, resulting in repressed E-cadherin expression. The precise understanding of nuclear PKM2 function suggests the potential for a model preventing cancer metastasis.

Author contributions: A.H., M.K., K.T., K.K., N.N., J.K., K.M., N.G., H.Y., Y.D., M.M., and H.I. designed research; A.H., M.K., and H.I. performed research; A.H., M.K., N.T., H.S., and H.I. contributed new reagents/analytic tools; A.H., M.K., J.K., N.G., M.M., and H.I. analyzed data; and A.H., M.K., N.T., H.S., K.T., K.K., N.N., J.K., K.M., N.G., M.M., and H.I. wrote the paper.

Conflict of interest statement: This work was supported in part by a Grant-in-Aid for Scientific Research from the Ministry of Education, Culture, Sports, Science, and Technology; a Grant-in-Aid from the Third Comprehensive 10-year Strategy for Cancer Control, Ministry of Health, Labor, and Welfare; a grant from the Kobayashi Cancer Research Foundation; a grant from the Princess Takamatsu Cancer Research Fund, Japan; a grant from the National Institute of Biomedical Innovation; and a grant from the Osaka University Drug Discovery Funds. A.H. is a research fellow of the Japan Society for the Promotion of Science. Partial support was received from Taiho Pharmaceutical Co., Ltd. (to J.K., M.M., and H.I.), Chugai Co., Ltd., Yakult Honsha Co., Ltd., Merck Co., Ltd., Takeda Science Foundation, and Takeda Medical Research Foundation (to M.K., N.N., M.M., and H.I.) through institutional endowments.

This article is a PNAS Direct Submission.

[1]A.H. and M.K. contributed equally to this work.

[2]To whom correspondence may be addressed. Email: mmori@gesurg.med.osaka-u.ac.jp or hishii@gesurg.med.osaka-u.ac.jp.

This article contains supporting information online at www.pnas.org/lookup/suppl/doi:10.1073/pnas.1407717111/-/DCSupplemental.

inhibiting epithelial cadherin (E-cadherin; encoded by *CDH1*) expression and acquiring mesenchymal markers. This process is physiologically important during embryogenesis and is required for in utero development. Given that PKM2 expression and EMT are common to both tumorigenesis and development, PKM2 may affect EMT within cancer cells. However, the significance of PKM2 during EMT or invasion is yet to be investigated.

In the present study, we demonstrate that PKM2 translocates into the nucleus during EMT and acts as a transcription cofactor that inhibits *CDH1* expression. PKM2 interacts with TGF-β–induced factor homeobox 2 (TGIF2), which recruits histone deacetylase 3 (HDAC3) to the promoter sequence of E-cadherin, thereby promoting histone H3 lysine 9 (H3K9) deacetylation and *CDH1* expression down-regulation.

Results

EMT Induction Elicits Nuclear Translocation of PKM2. For the induction of EMT, we cultured colon cancer cells in a medium with TGF-β1 and EGF, as described previously (Fig. 1*A*) (11–14). The SW480 cells changed morphology from epithelial to fibroblastic-like and spindle-shaped in a time-dependent manner (Fig. 1*B*). Consistent with this observation, *CDH1* transcript expression was suppressed, whereas the expression levels of the vimentin (*VIM*), zinc finger e-box binding homeobox 1 (*ZEB1*), and snail family zinc finger 2 (*SNAI2*) genes were increased (Fig. 1*C*). PK gene expression was induced in the EMT condition, with preferential expression of PKM2 compared with PKM1 (Fig. 1*D*). Western blot analysis indicated that the induction of EMT resulted in decreased *CDH1* expression, increased *VIM* expression, and up-regulated PKM2 (Fig. 1*E*). We confirmed that the expression and secretion of endogenous TGF-β1 was minimal in SW480 (Fig. S1 *A* and *B*).

To determine the intracellular localization of proteins, cytoplasmic and nuclear fractions were separated from the EMT-induced cells and Western blot analysis was performed. The data indicated that, although the EMT condition stimulated an increase in cytoplasmic PKM2, nuclear PKM2 was augmented compared with levels in the pre-EMT state (Fig. 1*F*). Immunocytochemistry and immunofluorescence intensity quantification confirmed the increase in nuclear PKM2 (Fig. S2 *A–D*). In addition, we confirmed that nuclear PKM2 was also increased in HCT116 cells under the same EMT condition (Fig. S2*E*) and that the expression of EMT markers was increased in murine *Pkm2* knock-in, compared with *Pkm1* knock-in, mesencymal cells, as well as other human cancer cells (Fig. S1 *C* and *D*).

Previous studies showed that EGF stimulation increased nuclear PKM2 (7) and indicated that cytoplasmic PKM2 functions with tetramer formation, whereas nuclear PKM2 functions with dimer formation. Given that the large hydrophobic hole at the nucleotide binding site is buried in tetrameric PKM2 structure, which becomes accessible in dimer form (15), the dimer formation may provide a protein binding ability. We studied the status of PKM2 during EMT and found that simultaneous stimulation by TGF-β1 and EGF, in comparison with either alone, resulted in increased expression of an ~120-kDa complex, corresponding to dimeric PKM2 (Fig. 1*G* and Fig. S3). The present study demonstrated that PKM2 nuclear translocation was stimulated in the EMT condition, suggesting a unique function of PKM2 in the nucleus.

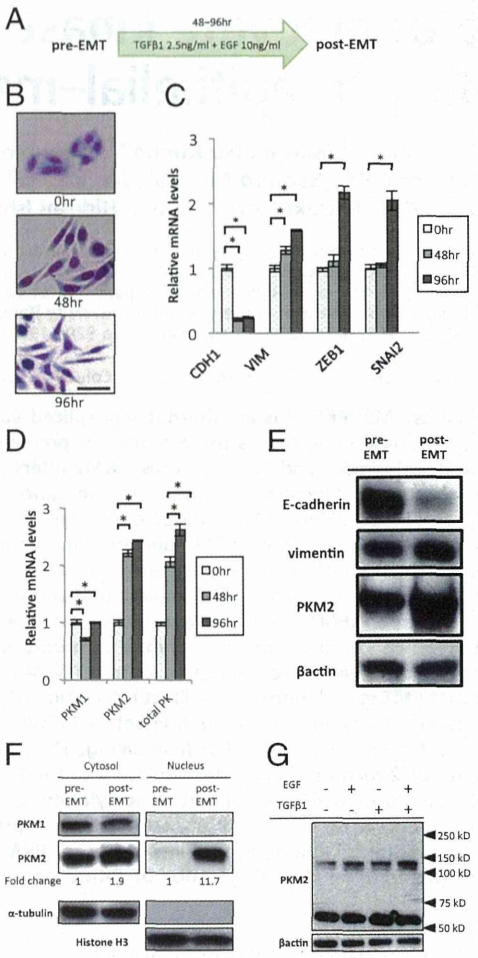

Fig. 1. PKM2 translocates into the nucleus during EMT. (*A*) Schematic representation of the procedure for EMT induction. The cells incubated for 48 h after seeding are defined as pre-EMT, and the cells cultured with 2.5 ng/mL TGF-β1 and 10 ng/mL EGF are defined as post-EMT. (*B*) Photomicrographs of the morphological change in SW480 cells. The cells were stained using the Diff-Quik Kit (Sysmex Corp.). The number of hours indicates the period since EMT induction was initiated. (Scale bar, 100 μm.) (*C*) Relative transcript (mRNA) levels of *CDH1*, *VIM*, *ZEB1*, and *SNAI2* after induction of EMT for 0, 48, and 96 h. The values at 0 h (pre-EMT) have been normalized to 1, and the data are expressed as fold. (*D*) Relative mRNA levels of PKM1, PKM2, and pyruvate kinase (total PK) after induction of EMT for 0, 48, and 96 h. (*E*) Western blot assays of E-cadherin, vimentin, and PKM2 expression in pre-EMT and post-EMT cells. Post-EMT cells were harvested at 72 h. (*F*) Western blot assays of PKM1, PKM2, α-tubulin, and histone H3 in nuclear and cytoplasmic lysates prepared from SW480 cells. With normalization to cytoplasmic tubulin or nuclear histone H3 blots, the relative intensities of PKM2 blots are shown in comparison with those in the pre-EMT condition. (*G*) SW480 cells were treated with dimethyl suberimidate for 30–60 min, immediately followed by whole cell lysis. The monomer and dimer states of PKM2 were analyzed by Western blot assay. Columns represent the average of at least three independent experiments; error bars represent the SD of the mean from triplicate results. $*P < 0.05$.

PKM2 Expression Is Required to Induce EMT. To investigate the causative role of PKM2 in EMT induction, we cultured cells with endogenous PKM2 inhibition by small interfering RNA (siRNA) knockdown (KD) under EMT conditions. We used the siRNA targeting system, which reportedly inhibits PKM2 without any off-target effects on other genes (16), and the results indicate that the most effective siRNA sequence could inhibit transcriptional and translational levels of PKM2, whereas those of PKM1 were increased (Fig. S4 *A* and *B*). PKM2 KD failed to induce spindle-shaped morphological changes under EMT conditions (Fig. 2*A*). Expression analysis indicated that PKM2 KD prevented *CDH1* down-regulation, although *VIM* expression persisted (Fig. 2*B*), suggesting a role for PKM2 in *CDH1* transcription. Fifty percent reductions in glucose or glutamine in the medium did not have significant effects on EMT marker expression (Fig. S5*A*), suggesting distinct effects on EMT and metabolism.

Western blot analysis indicated that PKM2 KD hindered *CDH1* loss and *VIM* gain compared with the control (Fig. 2*C*).

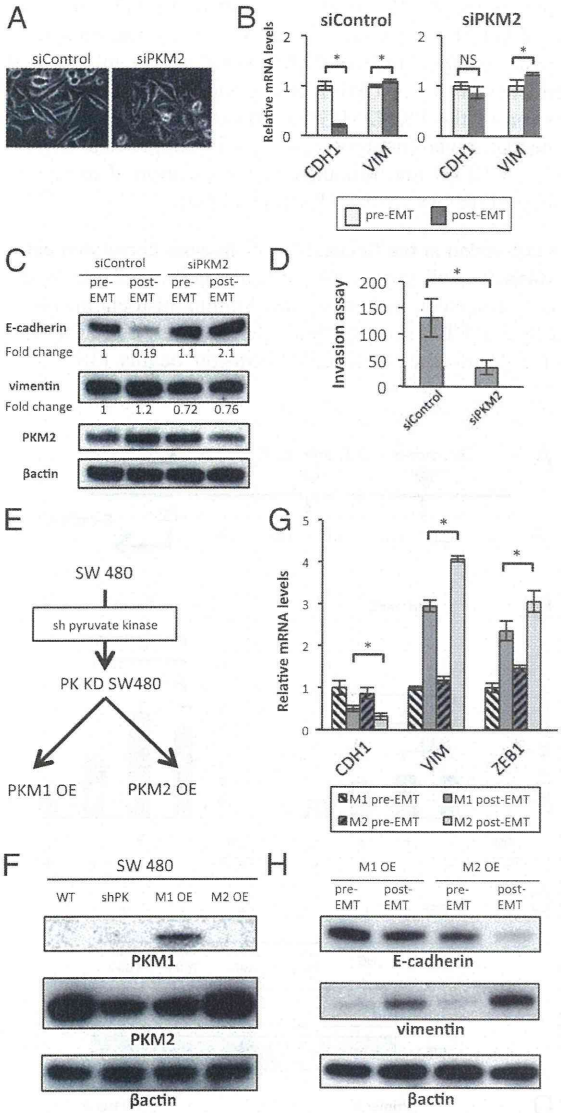

Fig. 2. PKM2 is required for EMT induction. (*A*) Phase-contrast photomicrographs of SW480 cells transfected with siControl or siPKM2 after EMT induction for 48 h. (*B*) Relative transcript (mRNA) levels of *CDH1* and *VIM* after EMT induction in cells transfected with siControl or siPKM2 for 48 h. (*C*) Western blot assays of E-cadherin, vimentin, PKM2, and β-actin expression in pre-EMT and post-EMT cells. Post-EMT cell samples were harvested at 72 h. With normalization to β-actin as a control, the relative intensities of E-cadherin and vimentin are shown in comparison with those in the control pre-EMT condition. Note that siPKM2 knockdown works efficiently in post-EMT cells. (*D*) Invasive behavior of SW480 cells treated with siControl or siPKM2. (*E*) Schematic procedure for establishing PKM1 OE or PKM2 OE SW480 cells. (*F*) Western blot assays of PKM1, PKM2, and β-actin expression in WT SW480 cells, cells stably expressing shRNA constructs targeting pyruvate kinase (shPK), and shPK cells overexpressing either PKM1 or PKM2 constructs. (*G*) Relative mRNA levels of *CDH1*, *VIM*, and *ZEB1* after EMT induction in PKM1 OE or PKM2 OE SW480 cells for 72 h. (*H*) Western blot assays of E-cadherin, vimentin, and β-actin expression in PKM1 OE and PKM2 OE cells. Post-EMT cell samples were harvested at 72 h. Column values = average of at least three independent experiments; error bars represent SD from the mean of triplicate experiments. $^*P < 0.05$.

Inhibition of EMT by PKM2 KD resulted in a significant reduction in in vitro cellular invasiveness (Fig. 2*D*). The assessment of mothers against decapentaplegic homolog 2 (SMAD2) and ERK, which are downstream effectors of TGF-β1 and EGF signaling, indicated that PKM2 KD disturbed the phosphorylation process (Fig. S5*B*).

To minimize the effect of an alternative exon and to focus on the function of PKM2 in the nucleus, we established PKM1- and PKM2-overexpressing (OE) cell lines (PKM1 and PKM2 OE in Fig. 2*E*). In brief, we transfected the cells with a small hairpin RNA (shRNA) vector targeting the common region in *PK* and then introduced an overexpression vector of PKM1 or PKM2 cDNA without a complementary sequence to the shRNA (Fig. 2*F*). We cultured the established cells in EMT-inducing conditions. The results demonstrated a greater decrease in *CDH1* expression and greater increase in *VIM* and *ZEB1* expression in PKM2 OE cells compared with that in PKM1 OE cells (Fig. 2*G* and Fig. S4*C*). Consistent results were obtained by Western blot analysis (Fig. 2*H*). These results indicate that PKM2 expression is necessary for EMT induction.

Nuclear PKM2 Binds to TGIF2 and Represses CHD1 Expression. Nuclear PKM2 reportedly binds to and phosphorylates STAT3 through its function as a protein kinase (15). The observation that nuclear PKM2 increased during EMT led us to consider the possibility that PKM2 may interact with other transcription factors. To validate this hypothesis, fractions pulled-down with the PKM2 antibody were subjected to LC-electrospray ionized TOF MS analyses. The result showed that nuclear PKM2 was coimmunoprecipitated with TGIF2 and that this binding was detectable when both EGF and TGFβ1 were added to the culture (Fig. 3*A*). These findings were confirmed by immunoprecipitation, followed by Western blot analysis (Fig. 3*B*). The EMT stimulation resulted in the significant increase of TGIF2 expression (Fig. S6*A*). TGIF2 KD did not show significant alterations of PKM2 expression regardless of EMT induction (Fig. 3*E* and Fig. S6*B*). We could not detect an association of PKM1 with TGIF2 in the nucleus (Fig. S7*A*), which further supports the cytoplasmic localization of PKM1 (Fig. 1*F*).

Melhuish et al. (17) revealed that TGIF2 is a transcriptional repressor that suppresses TGF-β–responsive gene expression by binding to TGF-β–activated SMADs. First, we performed TGIF2 KD, followed by EMT induction (Fig. 3*C* and Fig. S6*B*). TGIF2 KD enhanced the decrease in both the transcriptional and the translational levels of *CDH1* expression (Fig. 3 *D* and *E*). To analyze the difference in the effect of TGIF2 KD in cells expressing either PKM1 or PKM2, we performed TGIF2 KD on PKM1 OE and PKM2 OE cells, followed by EMT induction. Interestingly, the decrease in *CDH1* expression and increase in *VIM* expression were similar at the transcriptional and translational levels after EMT induction in both cell lines (Fig. 3 *F* and *G*). These results indicate that the augmented sensitivity to EMT induction in PKM2 OE cells is abrogated under TGIF2 suppression. These data further suggest that nuclear PKM2 responds to EMT stimulation and interacts with TGIF2 to mediate EMT induction downstream of PKM2.

PKM2 and TGIF2 Recruit HDAC3 to the *CDH1* Promoter to Repress Transcription. TGIF2 is a transcriptional factor that regulates TGF-β signal transduction (17). Based on the above findings, we hypothesized that TGIF2 could bind to the *CDH1* promoter and activate *CDH1* expression in the epithelial state. To examine this hypothesis, we performed a ChIP quantitative PCR (qPCR) assay using two sets of primers located in the *CDH1* promoter sequence region (Fig. 4*A*). We found depressed binding of TGIF2 to the *CDH1* promoter region during EMT (Fig. 4*B*).

TGIF2 can control transcription by recruiting HDAC in response to TGF-β signaling (17) and PKM2 can associate with HDAC3 in the nucleus (7). To investigate whether TGIF2 can bind to HDAC3 during EMT, we performed immunoprecipitation followed by Western blot analysis and found an association between TGIF2 and HDAC3 under EMT induction (Fig. 4*C* and

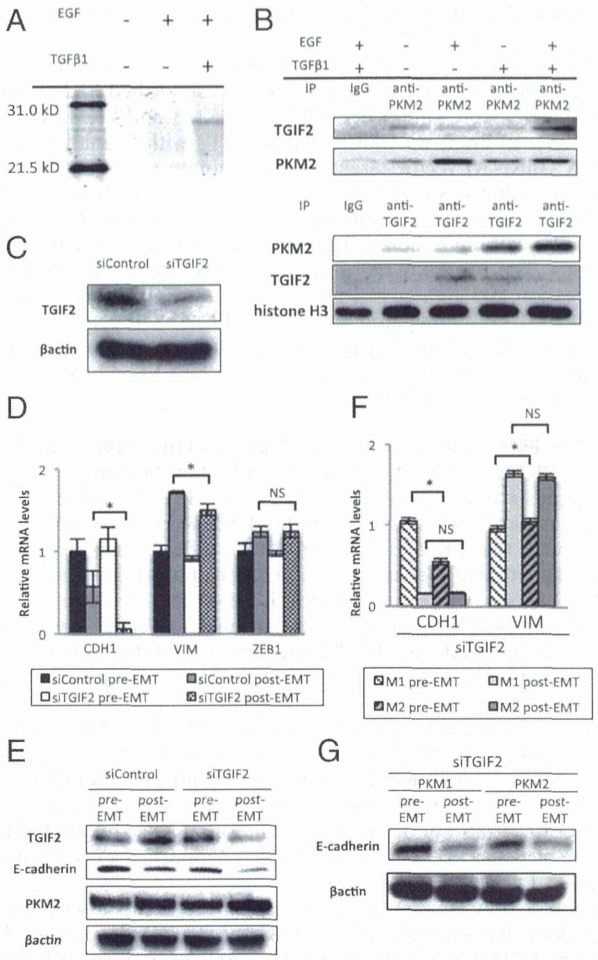

Fig. 3. Interaction between nuclear PKM2 and TGIF2 mediates EMT induction. (*A*) Polyacrylamide gel electrophoresis of proteins immunoprecipitated with anti-PKM2 antibody in the nucleic lysate of cells cultured under normal conditions, with EGF alone, or with TGF-β1 and EGF. The band detected in samples of cells stimulated with TGF-β1 and EGF was excised and analyzed by MS. (*B*) Western blot assays of immunoprecipitated samples of nucleic lysates with anti-PKM2 or anti-TGIF2 antibody. Samples were harvested after the cells were treated as indicated for 72 h. (*C*) Western blot assays of TGIF2 and β-actin expression in cells transfected with siControl or siTGIF2. (*D*) Relative transcript (mRNA) levels of *CDH1*, *VIM*, and *ZEB1* after induction of EMT in cells transfected with siControl or siTGIF2 for 72 h. (*E*) Western blot analysis of TGIF2, E-cadherin, PKM2, and β-actin expression in pre-EMT and post-EMT cells transfected with siControl or siTGIF2. Post-EMT samples were harvested at 72 h, when siRNA inhibition was profound. (*F*) Relative mRNA levels of *CDH1* and *VIM* after EMT induction in PKM1 OE and PKM2 OE cells. Post-EMT samples were harvested at 72 h. (*G*) Western blot analysis of E-cadherin and β-actin after EMT induction in PKM1 OE and PKM2 OE cells transfected with siTGIF2. Post-EMT samples were harvested at 72 h. Column values = average of at least three independent experiments; error bars represent SD from the mean of triplicate experiments. $^*P < 0.05$.

Figs. S7*B* and S8). To examine the acetylation status of histone H3 in the *CDH1* promoter region, we performed ChIP qPCR and found that binding of acetylated H3K9 to the *CDH1* promoter was decreased under EMT conditions (Fig. 4*D*). Furthermore, to understand how the PKM2–TGIF2–HDAC3 complex can bind to the *CDH1* promoter, additional ChIP qPCR analysis was performed. The data indicated that similar to the binding of TGIF2, the binding of PKM2 and HDAC3 to the *CDH1* promoter was reduced during EMT (Fig. S9 *A* and *B*). Given that the TGIF2 protein bound to PKM2 and HDAC3 during EMT (Figs. 3*B* and 4*C* and Fig. S7*B*), the present study demonstrates that nuclear PKM2 plays a role in the TGIF2-dependent control of CHD1 expression and that EGF induces formation of the PKM2–TGIF2–HDAC3 complex, followed by histone deacetylation, thus resulting in suppressed *CDH1* expression. TGF-β1 may modulate the association of this complex, although H3K9 was deacetylated (Fig. 5*D*).

PKM2 Expression in the Deepest Tumor Regions Correlated with CRC Metastasis. To investigate the clinical significance of PKM2 expression in cancer metastasis, we immunohistochemically analyzed clinical CRC samples. Staining was assessed in the deepest tumor regions where the CRC invasion begins (18, 19). The

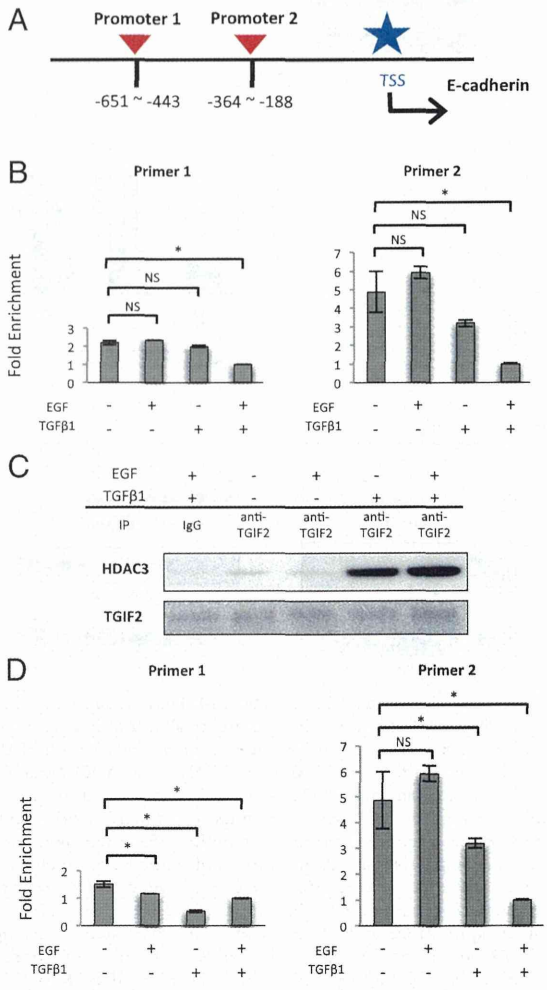

Fig. 4. TGIF2 binds to the CDH promoter and recruits HDAC3 during EMT. (*A*) Schematic diagram showing the positions of two sets of primers designed to cover the promoter region of the *CDH1* gene. (*B*) ChIP assays were performed with IgG and anti-TGIF2 antibody, followed by qPCR (mean ± SD, $n = 3$). ChIP samples were harvested from the nucleic lysate of SW480 cells treated as indicated for 72 h. (*C*) Western blot assays of immunoprecipitated samples of nucleic lysate with anti-TGIF2 antibody. Each sample was harvested after the cells were treated as indicated for 72 h. (*D*) ChIP assays were performed with IgG and anti-acetylated H3K9 antibody, followed by qPCR (mean ± SD, $n = 3$). ChIP samples were harvested from the nucleic lysate of SW480 cells treated as indicated for 72 h. Column values = average of at least three independent experiments; error bars represent SD from the mean of triplicate experiments. $^*P < 0.05$.

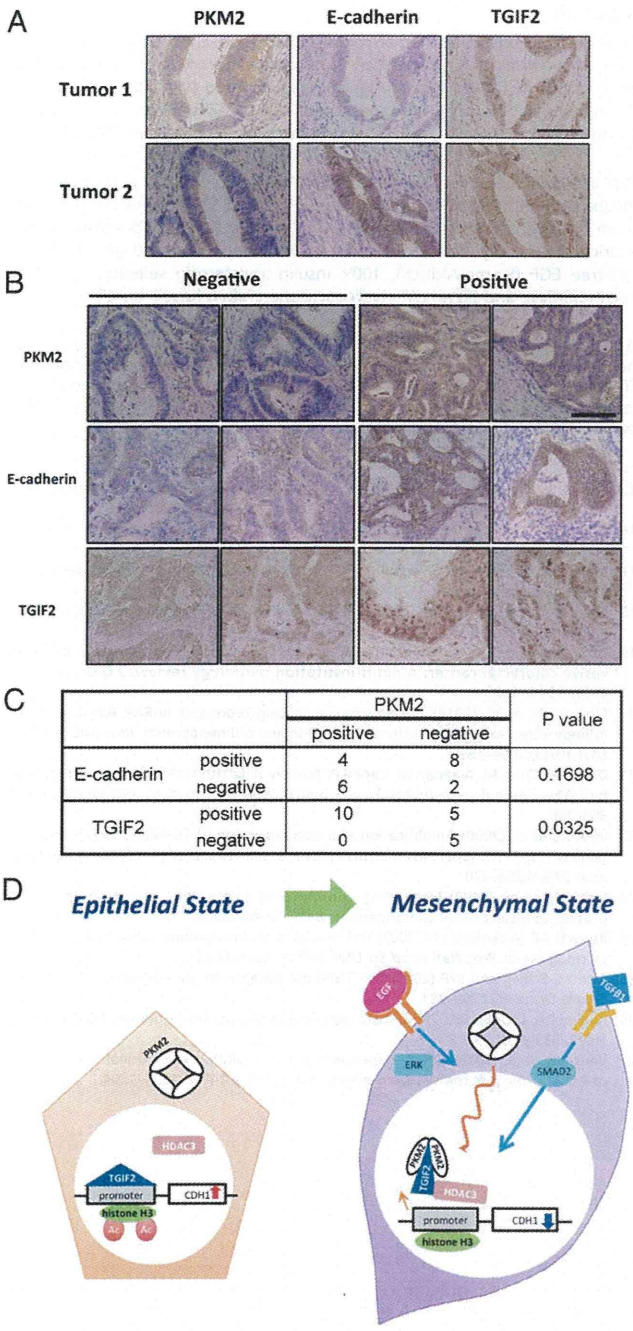

		PKM2 positive	PKM2 negative	P value
E-cadherin	positive	4	8	0.1698
	negative	6	2	
TGIF2	positive	10	5	0.0325
	negative	0	5	

Fig. 5. The immunohistochemistry. (*A*) Staining at the invasive front, showing an inverse correlation between PKM2, E-cadherin, and TGIF2 expression. (Scale bar, 100 μm.) (*B*) The representative cases are shown for staining for PKM2, TGIF2, and E-cadherin. Invasive fronts of tumors were stained by anti-PKM2, anti-E-cadherin, and anti-TGIF2 antibodies, and the intensities were assigned to positive and negative groups. With regard to TGIF2 staining, under the microscopic observation, cases with more than 50% of cells stained in nucleus were designated as positive, whereas the others were negative. (*C*) The 10 positive and 10 negative cases for cellular PKM2 were examined for nuclear TGIF2 and membranous E-cadherin. (*D*) Theoretical model illustrating the functional roles of PKM2 and TGIF2 in regulating *CDH1* transcription during EMT.

PKM2 staining intensities were assigned to positive and negative groups (Fig. 5 *A*–*C*). The correlations between PKM2 expression and clinicopathological factors are summarized in Table S1. PKM2-positive staining was significantly correlated with metastasis to lymph nodes and distant organs. To further understand the clinical significance of PKM2 in CRC, we analyzed the GSE17536 database of the gene expression array and patient prognosis. To study the specific effect of PKM2 in the array database, we analyzed expression of both PK and its splicing factor hnRNPA2, because hnRNPA2 stimulates the splicing to PKM2 (20, 21). As expected, cases with high PK and high hnRNPA2 expression showed a poorer prognosis than other groups; the difference in prognosis was apparent in stages III and IV with metastasis (Fig. S10 *A* and *B*). The data confirmed that PKM2 can enhance the ability of cancer cells to metastasize in primary cancer tissues.

Discussion

In the present study, we demonstrated that nuclear PKM2 interacts with TGIF2 during EMT, which is pivotal in promoting the transition into the mesenchymal cancer cell phenotype. Consequently, we propose a model for the nuclear PKM2 function in response to EMT stimulation (Fig. 5*D*). Under epithelial conditions, histone H3 is acetylated on the *CDH1* promoter region and *CDH1* is transcribed where TGIF2 should serve as an active transcription factor. Once the EMT signal stimulates transformation of the cancer cell, a PKM2 fraction enters the nucleus and associates with TGIF2. We assume that this association will alter the conformation of TGIF2 or its associated complexes, effectively loosening the binding between TGIF2 and the *CDH1* promoter sequence to allow the recruitment of HDAC3 and subsequent histone H3 deacetylation. *CDH1* expression is suppressed as a consequence of the downregulated promoter activity. In this context, nuclear PKM2 serves as a transcriptional cofactor regulating TGIF2 behavior.

Few reports have investigated the significance of TGIF2 in cancer. In ovarian cancer, TGIF2 is reportedly amplified and overexpressed (22), whereas a comparison between colorectal adenoma and colorectal carcinoma revealed that TGIF2 expression is increased only in the latter (23). Further, TGIF2 has been shown to interact with TGF-β–activated SMADs and be able to repress the activation of TGF-β–responsive transcription (17). The present study demonstrated that TGIF2 affects *CDH1* expression through the regulation of promoter activity in which TGIF2 is supposed to function as an activating transcription factor.

TGF-β1 is a multifunctional cytokine that has dual and opposing roles in controlling cell fate. In the early stages of cancer, TGF-β1 induces growth arrest and apoptosis, exerting tumor-suppressive effects, whereas in later stages, TGF-β1 enhances tumor progression by provoking a variety of malignancy-related responses, including EMT (24–26). This paradox remains unsolved despite numerous studies addressing the issue. However, based on the results in the present study, we propose that the interaction between PKM2 and TGIF2 may offer a plausible explanation. In normal cells, PK expression is exclusively shifted to PKM1, but on TGF-β signaling, TGIF2 can suppress transcription downstream of the SMAD signal. Conversely, in cancer cells abundantly expressing PKM2, PKM2 translocates and is bound to TGIF2 in the nucleus, thereby reversing TGF-β signal transduction. Further investigation is necessary to determine the significance of TGIF2 expression and the precise mechanism underlying this interaction.

Nuclear PKM2 forms a dimer and functions as a protein kinase, whereas cytoplasmic PKM2 forms a tetramer and functions as a pyruvate kinase (15). In the present study, the dimeric form of PKM2 was increased, suggesting that the protein kinase activity of PKM2 is enhanced during EMT. PKM2 translocates into the nucleus in response to variable signals, of which, the EGF–ERK pathway is the most investigated (7, 27). Interestingly, TGIF2 is phosphorylated in response to EGF signaling (17). Given that EGF induces nuclear translocation of PKM2, PKM2 may function as a dimeric protein kinase in the

nucleus, phosphorylating TGIF2. However, the phosphorylation status of TGIF2 was not addressed in our study. Gao et al. (15) demonstrated that PKM2 interacts with STAT3 to control downstream gene expression in SW480 cells. Thus, it is conceivable that the molecular interaction of PKM2 is highly context dependent, with cell fate determined by how nuclear PKM2 regulates gene expression.

PKM2 has both metabolic and nonmetabolic functions, which are essential in the cytoplasm and nucleus, respectively. Increasing evidence has suggested that nuclear PKM2 binds to numerous transcriptional factors, thereby conferring cells with advanced malignant potential. The present study determined that PKM2 significantly influences EMT induction by modulating *CDH1* expression, thus providing a molecular basis for EMT acquisition. Future cancer treatments may be able to target the inhibition of nuclear PKM2.

Methods

Cell Lines and Culture. The human colorectal cancer cell lines, SW480 and HCT116, were obtained from ATCC, and CaR-1 was obtained from JCRB. These cell lines were grown in DMEM (Sigma-Aldrich) supplemented with 10% (vol/vol) FBS (Thermo Fisher Scientific), 100 U/mL penicillin, and 100 U/mL streptomycin (Life Technologies) and grown at 37 °C in a humidified incubator with 5% CO_2.

EMT Induction. Cells were seeded at a concentration of 5.0×10^4 cells/mL and incubated in a humidified atmosphere (37 °C and 5% CO_2) in standard medium for 48 h, after which they were treated with TGF-β1 (2.5 ng/mL; Sigma-Aldrich). Next, they were incubated with MEM supplemented with 10 ng/mL FBS-free EGF (Sigma-Aldrich), 100× insulin-transferring selenium (ITS; Life Technologies), and 50 nmol/L hydrocortisone (Tokyo Kasei) for 48–96 h.

ACKNOWLEDGMENTS. We thank the members of our laboratories for helpful discussions; Idea Consultants, Inc. (Osaka, Japan) and Olympus Co. (Tokyo, Japan) for technical assistance; Lewis C. Cantley for providing the lentiviral shRNA and retroviral expression vector; and H. Miyoshi for providing the packaging plasmids.

1. Jemal A, et al. (2011) Global cancer statistics. *CA Cancer J Clin* 61(2):69–90.
2. Warburg O (1956) On the origin of cancer cells. *Science* 123(3191):309–314.
3. Vander Heiden MG, Cantley LC, Thompson CB (2009) Understanding the Warburg effect: The metabolic requirements of cell proliferation. *Science* 324(5930):1029–1033.
4. Christofk HR, et al. (2008) The M2 splice isoform of pyruvate kinase is important for cancer metabolism and tumour growth. *Nature* 452(7184):230–233.
5. Hacker HJ, Steinberg P, Bannasch P (1998) Pyruvate kinase isoenzyme shift from L-type to M2-type is a late event in hepatocarcinogenesis induced in rats by a choline-deficient/DL-ethionine-supplemented diet. *Carcinogenesis* 19(1):99–107.
6. Elbers JR, et al. (1991) Pyruvate kinase activity and isozyme composition in normal fibrous tissue and fibroblastic proliferations. *Cancer* 67(10):2552–2559.
7. Yang W, et al. (2011) Nuclear PKM2 regulates β-catenin transactivation upon EGFR activation. *Nature* 480(7375):118–122.
8. Luo W, et al. (2011) Pyruvate kinase M2 is a PHD3-stimulated coactivator for hypoxia-inducible factor 1. *Cell* 145(5):732–744.
9. Hanahan D, Weinberg RA (2011) Hallmarks of cancer: The next generation. *Cell* 144(5):646–674.
10. Weinberg RA (2008) Mechanisms of malignant progression. *Carcinogenesis* 29(6): 1092–1095.
11. Rees JR, Onwuegbusi BA, Save VE, Alderson D, Fitzgerald RC (2006) In vivo and in vitro evidence for transforming growth factor-beta1-mediated epithelial to mesenchymal transition in esophageal adenocarcinoma. *Cancer Res* 66(19):9583–9590.
12. Yokobori T, et al. (2013) Plastin3 is a novel marker for circulating tumor cells undergoing the epithelial-mesenchymal transition and is associated with colorectal cancer prognosis. *Cancer Res* 73(7):2059–2069.
13. Okada H, Danoff TM, Kalluri R, Neilson EG (1997) Early role of Fsp1 in epithelial-mesenchymal transformation. *Am J Physiol* 273(4 Pt 2):F563–F574.
14. Strutz F, et al. (2002) Role of basic fibroblast growth factor-2 in epithelial-mesenchymal transformation. *Kidney Int* 61(5):1714–1728.
15. Gao X, Wang H, Yang JJ, Liu X, Liu ZR (2012) Pyruvate kinase M2 regulates gene transcription by acting as a protein kinase. *Mol Cell* 45(5):598–609.
16. Goldberg MS, Sharp PA (2012) Pyruvate kinase M2-specific siRNA induces apoptosis and tumor regression. *J Exp Med* 209(2):217–224.
17. Melhuish TA, Gallo CM, Wotton D (2001) TGIF2 interacts with histone deacetylase 1 and represses transcription. *J Biol Chem* 276(34):32109–32114.
18. Lugli A, Karamitopoulou E, Zlobec I (2012) Tumour budding: A promising parameter in colorectal cancer. *Br J Cancer* 106(11):1713–1717.
19. Ueno H, et al. (2014) Novel risk factors for lymph node metastasis in early invasive colorectal cancer: A multi-institution pathology review. *J Gastroenterol* 49(9):1314–1323.
20. Clower CV, et al. (2010) The alternative splicing repressors hnRNP A1/A2 and PTB influence pyruvate kinase isoform expression and cell metabolism. *Proc Natl Acad Sci USA* 107(5):1894–1899.
21. David CJ, Chen M, Assanah M, Canoll P, Manley JL (2010) HnRNP proteins controlled by c-Myc deregulate pyruvate kinase mRNA splicing in cancer. *Nature* 463(7279): 364–368.
22. Imoto I, et al. (2000) Amplification and overexpression of TGIF2, a novel homeobox gene of the TALE superclass, in ovarian cancer cell lines. *Biochem Biophys Res Commun* 276(1):264–270.
23. Lips EH, et al. (2008) Integrating chromosomal aberrations and gene expression profiles to dissect rectal tumorigenesis. *BMC Cancer* 8:314.
24. Roberts AB, Wakefield LM (2003) The two faces of transforming growth factor beta in carcinogenesis. *Proc Natl Acad Sci USA* 100(15):8621–8623.
25. Tian M, Schiemann WP (2009) The TGF-beta paradox in human cancer: An update. *Future Oncol* 5(2):259–271.
26. Rahimi RA, Leof EB (2007) TGF-beta signaling: A tale of two responses. *J Cell Biochem* 102(3):593–608.
27. Yang W, et al. (2012) ERK1/2-dependent phosphorylation and nuclear translocation of PKM2 promotes the Warburg effect. *Nat Cell Biol* 14(12):1295–1304.